AD-A044 342 ILLINOIS UNIV AT URBANA-CHAMPAIGN COORDINATED SCIENCE LAB F/G 9/1
ANALYSIS OF INVERTED STRIP DIELECTRIC WAVEGUIDES AND PASSIVE DE--ETC(U)
JUL 77 R S RUDOKAS DAAB07-72-C-0259
UNCLASSIFIED R-774 NL

END
DATE FILMED
10-77
DDC

REPORT R-774 JULY, 1977 UILU-ENG 77-2221

COORDINATED SCIENCE LABORATORY

ANALYSIS OF INVERTED STRIP DIELECTRIC WAVEGUIDES AND PASSIVE DEVICES FOR MILLIMETER WAVES

RONALD STEVE RUDOKAS

UNIVERSITY OF ILLINOIS - URBANA, ILLINOIS

UNCLASSIFIED

SECURITY CLASSIFICATION OF THIS PAGE (When Data Entered)

REPORT DOCUMENTATION PAGE

READ INSTRUCTIONS BEFORE COMPLETING FORM

1. REPORT NUMBER
2. GOVT ACCESSION NO.
3. RECIPIENT'S CATALOG NUMBER

4. TITLE (and Subtitle)

ANALYSIS OF INVERTED STRIP DIELECTRIC WAVEGUIDES and Passive Devices for Millimeter Waves.

5. TYPE OF REPORT & PERIOD COVERED

Technical Report

6. PERFORMING ORG. REPORT NUMBER

R-774, UILU-ENG-77-2221

7. AUTHOR(s)

Ronald Steve Rudokas

8. CONTRACT OR GRANT NUMBER(s)

DAAB-07-72-C-0259

9. PERFORMING ORGANIZATION NAME AND ADDRESS

Coordinated Science Laboratory
University of Illinois at Urbana-Champaign
Urbana, Illinois 61801

10. PROGRAM ELEMENT, PROJECT, TASK AREA & WORK UNIT NUMBERS

11. CONTROLLING OFFICE NAME AND ADDRESS

Joint Services Electronics Program

12. REPORT DATE

July 1977

13. NUMBER OF PAGES

47

14. MONITORING AGENCY NAME & ADDRESS (if different from Controlling Office)

Master's thesis, 54p.

15. SECURITY CLASS. (of this report)

UNCLASSIFIED

15a. DECLASSIFICATION/DOWNGRADING SCHEDULE

16. DISTRIBUTION STATEMENT (of this Report)

Approved for public release; distribution unlimited

17. DISTRIBUTION STATEMENT (of the abstract entered in Block 20, if different from Report)

18. SUPPLEMENTARY NOTES

19. KEY WORDS (Continue on reverse side if necessary and identify by block number)

Millimeter Waves
Inverted Strip Dielectric Waveguides

20. ABSTRACT (Continue on reverse side if necessary and identify by block number)

The analysisofthe propagation characteristics of homogeneous and heterogeneous inverted strip dielectric waveguide is presented. Using the heterogeneous guide a ring resonator, distributed directional coupler and beam splitter type directional coupler are described and analyzed. Experimental measurements verifying the analytical results are included.

DD FORM 1 JAN 73 1473 EDITION OF 1 NOV 65 IS OBSOLETE

097700

UNCLASSIFIED

SECURITY CLASSIFICATION OF THIS PAGE (When Data Entered)

UILU-ENG 77-2221

ANALYSIS OF INVERTED STRIP DIELECTRIC WAVEGUIDES AND PASSIVE FOR MILLIMETER WAVES

by

Ronald Steve Rudokas

This work was supported in part by the Joint Services Electronics Program (U.S. Army, U.S. Navy and U.S. Air Force) under Contract DAAB-07-72-C-0259.

ANALYSIS OF INVERTED STRIP DIELECTRIC WAVEGUIDES AND PASSIVE DEVICES FOR MILLIMETER WAVES

BY

RONALD STEVE RUDOKAS

B.S. University of Illinois, 1975

THESIS

Submitted in partial fulfillment of the requirements
for the degree of Master of Science in Electrical Engineering
in the Graduate College of the
University of Illinois at Urbana-Champaign, 1977

Thesis Adviser: Professor Raj Mittra

Urbana, Illinois

ACKNOWLEDGEMENT

The author wishes to express his sincerest thanks to Professor Raj Mittra and Dr. Tatsuo Itoh who contributed the original theoretical work on which this thesis is based. In particular I would like to thank Dr. Itoh for his invaluable guidance.

TABLE OF CONTENTS

INTRODUCTION

In an effort to find low cost methods of implementing millimeter wave circuits much energy has gone into the study of dielectric guiding structures. For many applications, this type of guide seems ideal from the standpoint of expense alone.

In Table 1, comparisons are made between metal, microstrip, insular and inverted strip guides [7]. Aside from electrical characteristics, dielectric guides in general are less expensive in terms of materials and fabrication. The inverted strip guide, first described by Itoh [11], may be constructed with losses approaching that of a metal waveguide. A cross section of this guide is shown in Figure 1a. This type of dielectric guide exhibits a number of desirable features.

a) Low loss - Figure 1b shows a plot of the relative field distribution as a function of y at $x = 0$. Since most of the energy is concentrated in the region around $x \approx 0$ and $y = h$, conductor loss and loss due to imperfections of the dielectric wall, at $x = \pm w/2$, are minimized. Losses at the ε_1, ε_2 interface are minimized since the materials are in contact and plastic flow, of the dielectrics, eliminates irregularities and air gaps.

Table 1

COMPARISON OF METAL, MICROSTRIP AND

DIELECTRIC WAVEGUIDES

DESCRIPTION	FREQUENCY (GHz)	λg (cm)	w (cm)	t (cm)	ATTENUATION (db/cm)
INVERTED STRIP WAVEGUIDE (Fused Quartz on Teflon, Multimode)	60	.500	.4	.317	(a)
	90	.333	.4	.317	(a)
INSULAR WAVEGUIDE (Alumina on Polyethylene	60	.237	.134	.013	.055
	90	.158	.090	.009	.095
MICROSTRIP (Gold on Fused Quartz)	60	.302	.027	.014	.154
	90	.201	.018	.009	.280
METAL WAVEGUIDE (Silver Plated)	60	.669	.376		.015
	90	.441	.245		.030

(a) Could not be detected using 10 cm "slotted" guide (<.1 db/cm)

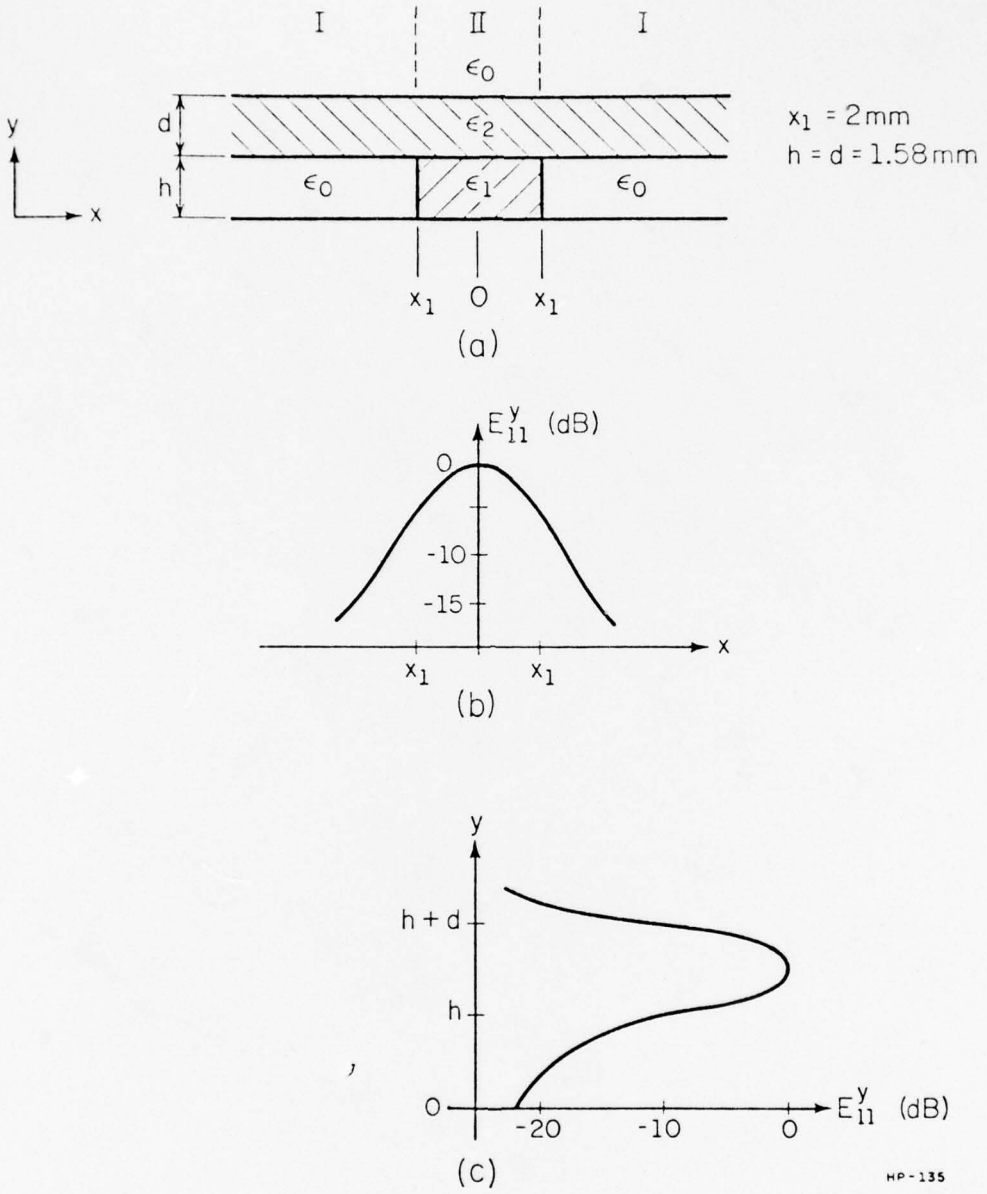

Figure 1. (a) Structure of the uncoupled inverted strip guide.
(b) Relative field distribution along the X axis.
(c) Relative field distribution along the Y axis.

b) The ground plane is readily available as a mechanical support, dc bias return, and heat sink for the guide and active devices placed in the guide.

c) The inverted strip guide, in the millimeter wave region, has dimensions on the order of 2-4 mm. This allows accurate and inexpensive fabrication in comparison to microstrip or metal waveguide.

d) Materials for the inverted strip guide are relatively inexpensive.

Analysis of the inverted strip (IS) guide is based on the concept of effective dielectric constants [3]. A theoretical analysis of the IS guide, distributed directional coupler, beam splitter type directional coupler and ring resonator will be presented with numerical results. Experimental results, for devices constructed for operation in the 80 GHz range, will also be presented.

CHAPTER II

THEORETICAL ANALYSIS

1. Maxwell's Equations as Applied to a Rectangular Dielectric Waveguide

A direct solution of Maxwell's Equations, as applied to the inverted strip dielectric waveguide, is extremely difficult since we do not have a separable geometry. The problem may be approached by recognizing that two independent sets of modes will propagate in the guide and applying the method of effective dielectric constants as developed by Knox and Toulios [3].

The two propagating field configurations, E_y^{pq} and E_x^{pq} are hybrid in nature, unlike the simple transverse magnetic or transverse electric modes found in rectangular metal waveguide [4]. For the E_y^{pq} modes the principal component of the electric field is along the y axis, where we have chosen the x and y directions as being horizontal and vertical. The superscripts p and q indicate the number of extrema in the x and y directions. Fundamental modes for this type of guide are the E_y^{11} and E_x^{11} modes.

Maxwell's equations may be written in a simple form using the scalar potentials ϕ^h and ϕ^e [5]. Using these potentials Maxwell's equations become:

$$E_x = \frac{1}{\varepsilon_r(y)} \frac{\partial^2 \phi^e}{\partial y \partial x} + \omega \mu K_z \phi^h \qquad \text{Eq 1}$$

$$E_y = \frac{1}{\varepsilon_r(y)} \left(K_z^2 - \frac{\partial^2}{\partial x^2} \right) \phi h \qquad \text{Eq 2}$$

$$E_z = \frac{-jK_z}{\varepsilon_r(y)} \frac{\partial \phi^e}{\partial y} - j\mu\omega \frac{\partial \phi^h}{\partial x} \qquad \text{Eq 3}$$

$$H_x = -\omega \varepsilon K_z \phi^e + \frac{\partial^2 \phi^h}{\partial y \partial x} \qquad \text{Eq 4}$$

$$H_y = \left(K_z^2 - \frac{\partial^2}{\partial x^2} \right) \phi h \qquad \text{Eq 5}$$

$$H_z = j \omega \varepsilon \frac{\partial \phi^e}{\partial x} - j K_z \frac{\partial \phi^h}{\partial y} \qquad \text{Eq 6}$$

where

ε = permitivity of free space

$\varepsilon_r(y)$ = relative dielectric constant in region of application

μ = permeability

ω = radian frequency

k_z = propagation constant in z direction

In reviewing the above equations we note that ϕ^e has a dominant contribution to the E_y^{pq} modes and ϕ^h has a dominant contribution to the E_x^{pq} modes. A good approximation to the fields for the E_y^{pq} modes may be obtained by setting ϕ^e equal to zero. Only the E_x^{pq} modes will be considered in the following analysis. This results in no loss of generality since the solutions for either set of modes are virtually identical. From a practical standpoint, the inverted strip guide is most likely to be excited from rectangular metal waveguide, Figure 8, in which

the dominant mode is the TE_{01} mode. In the transition from metal to dielectric guide there will be some high order E_y^{pq} and E_x^{pq} modes generated at the junction, because of the discontinuity, but most of the energy will propagate in the lower order E_y^{pq} modes.

2. Application of the Method of Effective Dielectric Constant

We will use an extension of the method of effective dielectric constants, as developed by Knox and Toulios [3], to perform a simple analysis of the inverted strip dielectric waveguide. Throughout the analysis we assume all materials are perfect and lossless.

Considering the more general case of the coupled transmission line (Figure 2) we note that the transmission line may be split into five regions. These five regions consist of either a two layer dielectric slab on a ground plane (region II), or a dielectric slab suspended above the ground plane (region I). If each region, alone, is extended to $\pm \infty$ in the x direction, each may be considered as a simple multilayer slab waveguide. By matching tangential magnetic and electric fields at each interface the propagation constant, in the y direction, may be determined for regions I and II. Each region may then be modeled by a homogeneous region with a dielectric constant chosen such that the propagation constant is identical to that of the original structure. This dielectric constant is the effective dielectric constant.

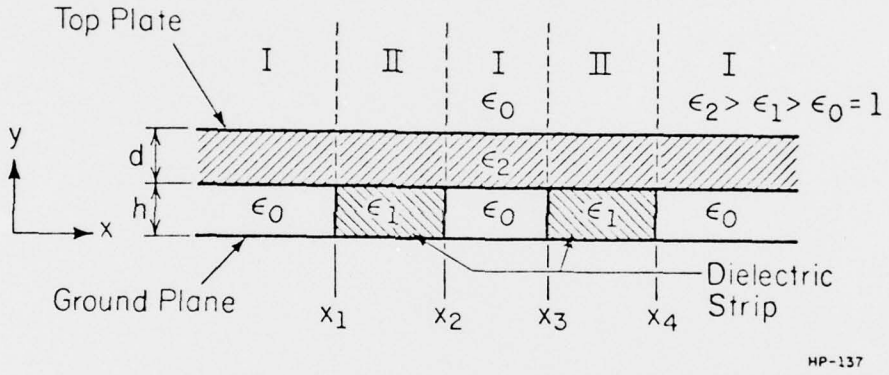

Figure 2. Cross section of the coupled inverted strip guide.

Having found the effective dielectric constant of each region we model the original structure by a multilayer slab waveguide (Figure 3), where we have substituted the proper effective dielectric constants for regions I and II. This has allowed us to remove the y dependence from further calculations. Matching tangental electric and magnetic fields at each interface, in Figure 3, we determine the propagation constant in the z direction. This will be a close approximation to the propagation constant of the original structure.

3. Derivation of the Eigenvalue Equations

a) Regions I and II

Regions I and II are modeled by homogeneous regions, of the proper dielectric constant, in determining the propagation constant for the original structure. Since we are only interested in a solution for the E_y^{pq} modes, ϕ^h may be set equal to zero in equations 1 through 6. Taking the more general case of two dielectric slabs of dielectric constant, ε_1 and ε_2, on a ground plane (Figure 4) we match tangenital fields at each interface to determine the propagation constant in the y direction. From Maxwell's equations the relationships between the tangenital fields H_x and E_z and the scalar potential ϕ^e are:

$$E_z \sim \frac{1}{\varepsilon_r(y)} \frac{\partial \phi^e}{\partial y} \qquad \text{Eq 7}$$

$$H_x \sim \phi^e \qquad \text{Eq 8}$$

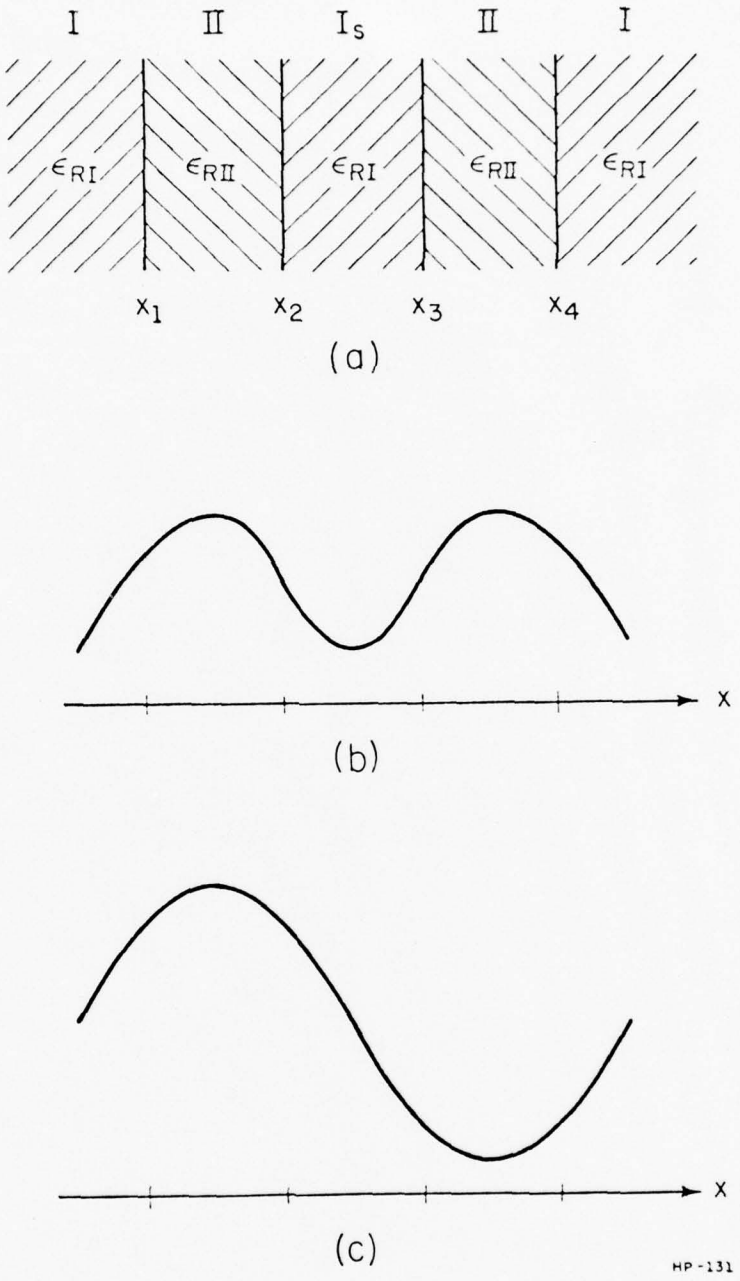

Figure 3. (a) Model of the inverted strip guide using effective dielectric constants.
(b) Relative field distribution for the even mode of the inverted strip guide.
(c) Relative field distribution for the odd mode of the inverted strip guide.

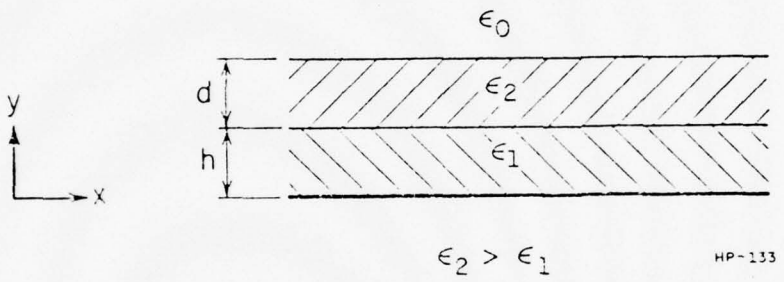

Figure 4. Structure used for effective dielectric constant calculation of region II.

We know that most of the energy in the slab guide will propagate in the region of higher dielectric constant. Therefore we assume a sinusoidally varying field distribution in ε_2, a decaying field above ε_2, and either a decaying or sinusoidal field in ε_1. The relative field distributions as a function of x are:

$$\phi^e(y) = A\ COSH(\eta_1 y) \qquad y < h \qquad \text{Eq 9}$$

$$\phi^e(y) = B\ COS[K_y(y-h)] + C\ SIN\ [K_y(y-h)] \qquad h < y < h+d \qquad \text{Eq 10}$$

$$\phi^e(y) = D\ e^{-\eta_3(y-h+d)} \qquad y > h+d \qquad \text{Eq 11}$$

where η_1 and η_3 are attenuation constants in their respective regions. Writing $\phi^e(y)$, for $y < h$, as a COSH function allows η_1 to assume either real or imaginary values corresponding to either a decaying or sinusoidal field. η_3 may only assume positive real values to insure that the field decays to zero as y goes to infinity.

Applying continuity of tangenital fields at each interface the eigenvalue equation is easily obtained.

$$K_y\ \varepsilon_1\ \varepsilon_2\ \eta_3\ COSH(\eta_1 h)\ COS(K_y d) +$$
$$\varepsilon_2^2\ \eta_1 \eta_3 SINH(\eta_1 h)\ SIN(K_y d) -$$
$$K_y^2\ \varepsilon_1\ COSH(\eta_1 h)\ SIN(K_y d) +$$
$$K_y\ \varepsilon_2 \eta_1\ SINH(\eta_1 h)\ COS(K_y d) = 0 \qquad \text{Eq 12}$$

Setting A, in Equation 9, equal to 1 the relative field distribution, as a function of y, becomes:

$$\phi^e(y) = \mathrm{COSH}(\eta_1 y) \qquad y < h \qquad \text{Eq 13}$$

$$\phi^e(y) = \mathrm{COSH}(\eta_1 y)\ \mathrm{COS}(K_y[y-h]) +$$

$$\frac{\eta_1\ \varepsilon_2}{K_y\ \varepsilon_1}\ \mathrm{SINH}(\eta_1 h)\ \mathrm{SIN}(K_y[y-h]) \qquad h < y < h+d \qquad \text{Eq 14}$$

$$\phi^e(y) = \left\{ \mathrm{COSH}(\eta_1[h+d])\ \mathrm{COS}(K_y d) + \right.$$

$$\left. \frac{\eta_1\ \varepsilon_2}{K_y\ \varepsilon_1}\ \mathrm{SINH}(\eta_1[h+d])\ \mathrm{SIN}(K_y d) \right\}$$

$$\varepsilon^{-\eta_3(y-h-d)} \qquad y > h+d \qquad \text{Eq 15}$$

Using the dispersion relation

$$K_z^2 = \varepsilon_o K_o^2 + \eta_3 = \varepsilon_2 K_o^2 - K_y^2 =$$

$$\varepsilon_1 K_o^2 + \eta_1^2 \qquad \text{Eq 16}$$

and the eigenvalue equation η_1, η_3 and k_y can be determined. Equation 16 is derived from a solution of the wave equation using the separation of variables technique [5]. Using these values in equations 13-15 the field distribution as a function of y can be plotted (Figure 1c).

The effective dielectric constant is defined:

$$K_z^2 = \varepsilon_{RII} K_o^2 \qquad \text{Eq 17}$$

where ε_{RII} is the effective dielectric constant of region II. Using equation 16:

$$\varepsilon_{RII} = \varepsilon_2 - \frac{K_y^2}{K_o^2} \qquad \text{Eq 18}$$

If ε_I in region II is set equal to ε_0 we obtain the slab waveguide of region I. Making the same substitution in Equations 9 through 18 we obtain the eigenvalue equation for region I.

$$K_y \varepsilon_2 \eta_1 \cos(K_y d)\,[1 + \tanh(\eta_1 h)] - K_y^2 \cos(K_y d) + \varepsilon_2^2 \eta_1^2 \tanh(\eta_1 h) \sin(K_y d) = 0 \qquad \text{Eq 19}$$

Setting A equal to 1 in equations 9 through 10 and making the same substitution as before the relative field distributions for region I are written as:

$$\phi^e(y) = \cosh(\eta_1 y) \qquad y < h \qquad \text{Eq 20}$$

$$\phi^e(y) = \cosh(\eta_1 h) \cos[K_y(y-h)] + \frac{\eta_1 \varepsilon_2}{K_y} \sinh(\eta_1 h) \sin[K_y(y-h)] \qquad h < y < h+d \qquad \text{Eq 21}$$

$$\phi^e(y) = \left\{ \cosh(\eta_1 h) \cos(K_y d) + \frac{\eta_1 \varepsilon_2}{K_y} \sinh(\eta_1 h) \sin(K_y d) \right\} e^{-\eta_1 (y-h-d)} \qquad y > h+d \qquad \text{Eq 22}$$

where, the attenuation constant, η_1, is taken to be real positive for confined fields. Using the dispersion relation for this region:

$$K_z^2 = \varepsilon_o K_o^2 + \eta_1^2 = \varepsilon_2 K_o^2 - K_y^2 \qquad \text{Eq 23}$$

the effective dielectric constant is:

$$\varepsilon_{RI} = \varepsilon_{2} - \frac{K_y^2}{K_o^2} \qquad \text{Eq 24}$$

b) Derivation of the Propagation Constant

Using the effective dielectric constants calculated in the previous section we can construct a model of the original structure by replacing each region by its respective effective dielectric constant as in Figure 3. The guide is assumed to be infinite in the ± x and y directions, therefore the fields will vary only as a function of x. Since ε_{RII} will always be greater than ε_{RI} we assume that most of the energy will propagate in regions II where there is a sinusoidal field variation. In region I a hyperbolic field distribution is assumed while in regions I we have an exponentially decaying field.

Matching tangential fields at each of the four boundaries results in a fairly cumbersome solution. In this complete solution two sets of propagating modes, the even and odd modes, may be recognized. In order to simplify the computation and interpretation of the solution we will formulate eigenvalue equations that contain only the desired solutions. Noting the symmetry of the even and odd modes (Figure 3a, 3b) with respect to the x-axis; we place an electric wall at x = 0 for the even modes and a magnetic wall at x = 0 for the odd modes.

For the even modes the tangential fields E_x and H_z are matched at each interface of Figure 5a. From equations 1 and 6 the relationship between these components and ϕ^e are:

$$E_y \sim \phi^e \qquad \text{Eq 25}$$

$$H_z \sim \frac{\partial \phi^e}{\partial x} \qquad \text{Eq 26}$$

Because of the electric wall at x = 0

$$E_y(0) = 0 \qquad \text{Eq 27}$$

Taking note of equation 27, we assume field distributions as a function of x:

$$\phi^e(x) = A\ \mathrm{SINH}(\xi x) \qquad x < x_1 \qquad \text{Eq 28}$$

$$\phi^e(x) = B\ \mathrm{COS}[k_x(x-x_1)] + C\ \mathrm{SIN}[K_y(x-x_1)] \qquad x_1 < x < x_2 \qquad \text{Eq 29}$$

$$\phi^e(x) = D\ e^{-\xi(x-x_2)} \qquad \text{Eq 30}$$

Where ξ is the attenuation constant in regions I_s and I. Matching fields at each interface and applying the dispersion relation:

$$K_z^2 = \varepsilon_{RI} K_o^2 + \xi^2 = \varepsilon_{RII} K_o^2 - K_x^2 \qquad \text{Eq 31}$$

we obtain the eigenvalue equation for even modes:

$$[\xi^2\ \mathrm{COSH}(\xi x_1) - K_x^2\ \mathrm{SINH}(\xi x_1)]\ \mathrm{SIN}[K_x(x_2-x_1)] + E_x\xi\,[\mathrm{COSH}(\xi x_1) + \mathrm{SINH}(\xi x_1)]\ \mathrm{COS}(K_x(x_2-x_1)] = 0 \qquad \text{Eq 32}$$

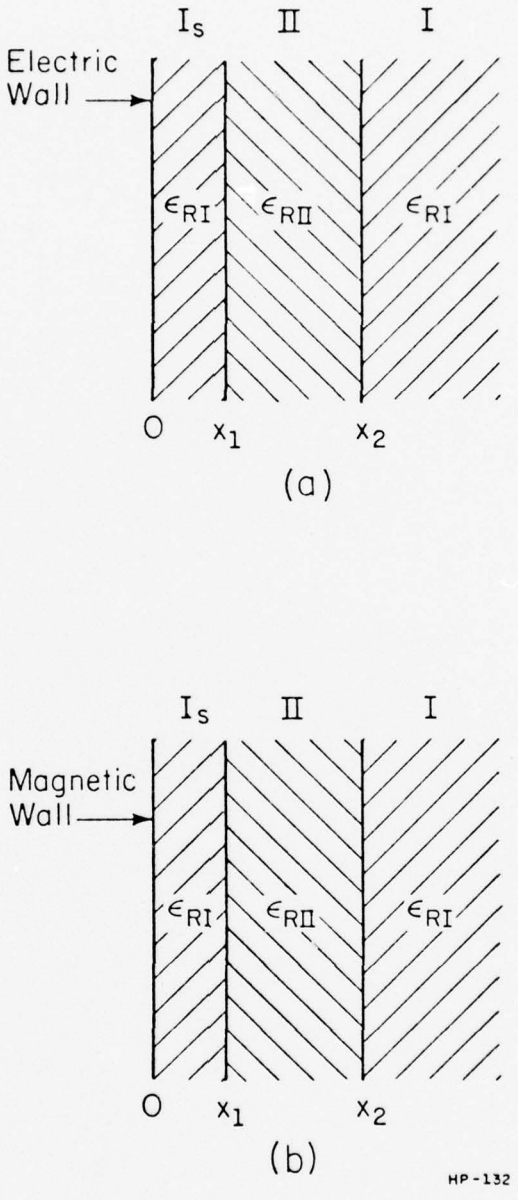

Figure 5. Structure used for derivation of the eigenvalue equations:
(a) Even modes.
(b) Odd modes.

ξ must be real positive for confined fields.

For the odd modes H_z is equal to zero at x = 0, (Figure 5b), because of the magnetic wall. Substituting

$$\phi^e(x) = \text{COSH}(\xi x) \qquad x < x_1 \qquad \text{Eq 33}$$

for equation 28 in the even mode solution we may use the same procedure to obtain the eigenvalue equation for odd modes.

$$[\xi \text{SINH}(\xi x_1) - K_x^2 \text{ COSH}(\xi x_1)] \text{ SIN}[K_x(x_2 - x_1)] +$$
$$[K_x \text{ SINH}(\xi x_1) + K_x \xi \text{ COSH}(\xi x_1)] \text{ COS } (K_x(x_2 - x_1)] = 0$$
$$\text{Eq 34}$$

c) Derivation of the Propagation Constant for the Uncoupled Guide

The uncoupled guide is shown in Figure 6a. Making the same observations as before we write the fields as:

$$\phi^e(x) = A\, e^{\xi(x-x_1)} \qquad x < x_1 \qquad \text{Eq 35}$$

$$\phi^e(x) = B \text{ COS } [K_x(x-x_1)] + C \text{ SIN}[K_x(x-x_1)]$$
$$x_1 < x < x_2 \qquad \text{Eq 36}$$

$$\phi^e(x) = D\, e^{-\xi(x-x_2)} \qquad x > x_2 \qquad \text{Eq 37}$$

Applying equations 25 and 26, and matching tangetial fields we obtain the eigenvalue equation for the uncoupled guide.

$$(K_x^2 - \xi^2) \text{ SIN } [K_x(x_2 - x_1)] - 2\xi K_x \text{ COS}[K_x(x_2 - x_1)] = 0$$
$$\text{Eq 38}$$

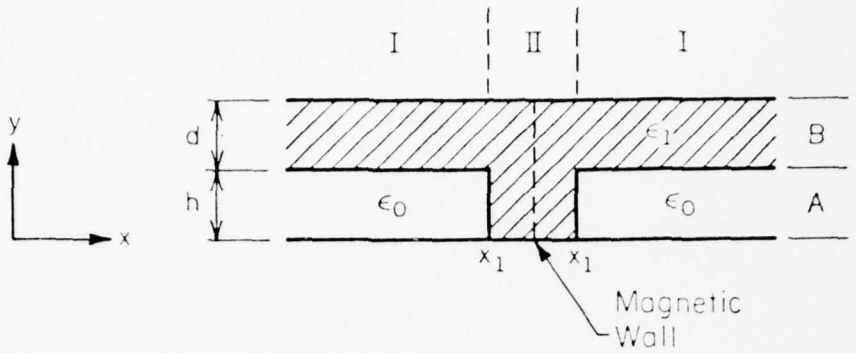

(a)

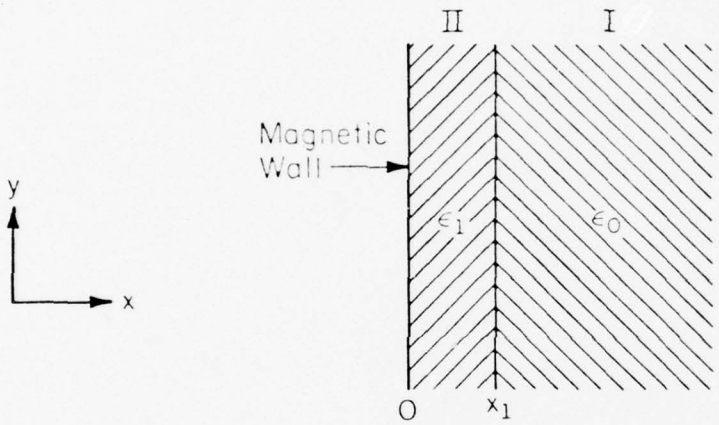

(b)

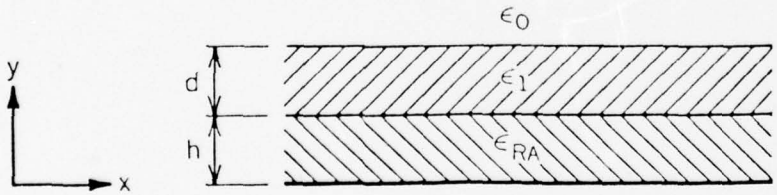

(c)

Figure 6. (a) Uncoupled homogeneous inverted strip guide.
(b) Structure for derivation of the effective dielectric constant in region A.
(c) Structure for derivation of the field distribution as a function of Y.

The first solution of each eigenvalue equation corresponds to the E_y^{11} mode of the even, odd or uncoupled field configurations. For higher order modes the Mth solution of the y directed eigenvalue equations (Equations 13 and 19) and the Nth solution of the x directed eigenvalue equations (Equations 31, 34 and 38) correspond to the E_y^{mn} propagating mode.

d) Extension of Analysis to a Homogeneous Guide

A guide with properties similar to the inverted strip guide may be constructed using a homogeneous structure rather than the heterogeneous structure of the inverted strip guide. This guide is structurally the same as that in Figure 1 with ε_1 set equal to ε_2 (Figure 6a).

Analysis to determine the propagation characteristics and field distribution as a function of x is similar to the preceding analysis with $\varepsilon_1 = \varepsilon_2$. In region I the y directed egeinvalue equation will be identical to Equation 19 found in section 3a. When $\varepsilon_1 = \varepsilon_2$ region II becomes a single layer slab waveguide. The field variation as a function of y is written in terms of a cosine in the dielectric and a decaying exponential above the dielectric.

$$\phi^e(y) = A\ COS(K_y y) \qquad y < h+d \qquad \text{Eq 39}$$

$$\phi^e(y) = B\ e^{-\eta(y-h+d)} \qquad y < h+d \qquad \text{Eq 40}$$

where η represents the attenuation constant of the dielectric region in the y direction. Matching tangential fields at

each interface we obtain the eigenvalue equation for region II of the homogeneous guide:

$$K_y \varepsilon_o \, SIN(K_y[h+d]) - \eta\varepsilon_1 \, COS(K_y[h+d]) = 0 \qquad \text{Eq 41}$$

Using Equation 41 and the dispersion relation

$$K_{z_{II}} = \varepsilon_1 K_o^2 - K_y^2 = \varepsilon_o K_o^2 + \eta^2 \qquad \text{Eq 42}$$

we can determine K_y. As before we can use K_y to define an effective dielectric constant for region II.

$$\varepsilon_{RII} = \varepsilon_1 - \frac{K_y^2}{K_o^2} \qquad \text{Eq 43}$$

Determination and characterization of the uncoupled, even, and odd mode propagation constants is identical to that of the heterogenous guide.

In order to determine the field variation as a function of y, in region II, we must consider the effects of the adjacent regions.

The guide may be modeled by two horizontal regions, A and B, of effective dielectric constant ε_A and ε_1. Applying the same type of analysis to Regions A and B as was applied to regions I and II, we arrive at the layered structure in Figure 6c. The effective dielectric constant of region B is ε_1, for region A we use Figure 6b to determine the effective dielectric constant.

Matching tangential fields E_y and H_z at each interface we find the eigenvalue equation:

$$\eta \cos(K_x x_1) - K_x \sin(K_x x_1) = 0 \qquad \text{Eq 44}$$

where η represents the attenuation constant and K_x is the propagation constant in the x direction. Using equation 44 with the dispersion relation

$$K_z^2 = \varepsilon_1 K_o^2 - K_x^2 = \varepsilon_o K_o^2 + \eta^2 \qquad \text{Eq 45}$$

the effective dielectric constant for region A is:

$$\varepsilon_{RA} = \varepsilon_1 - \frac{K_x^2}{K_o^2} \qquad \text{Eq 46}$$

In order to determine the vertical field distribution the two layer dielectric slab model, constructed with dielectric constants ε_1 and ε_{RA}, is analyzed in the same manner as region II.

e) Numerical Calculation of Propagation Characteristics

Numerical solutions were obtained by calculating the roots of the eigenvalue equation using a combination of the bisection method and the tangent method. Figures 7 and 8 show the results of these calculations for a guide of typical dimensions.

4. Analysis of the Distributed Directional Coupler

A simple distributed coupler consists of a section of coupled inverted strip guide of length ℓ and separation

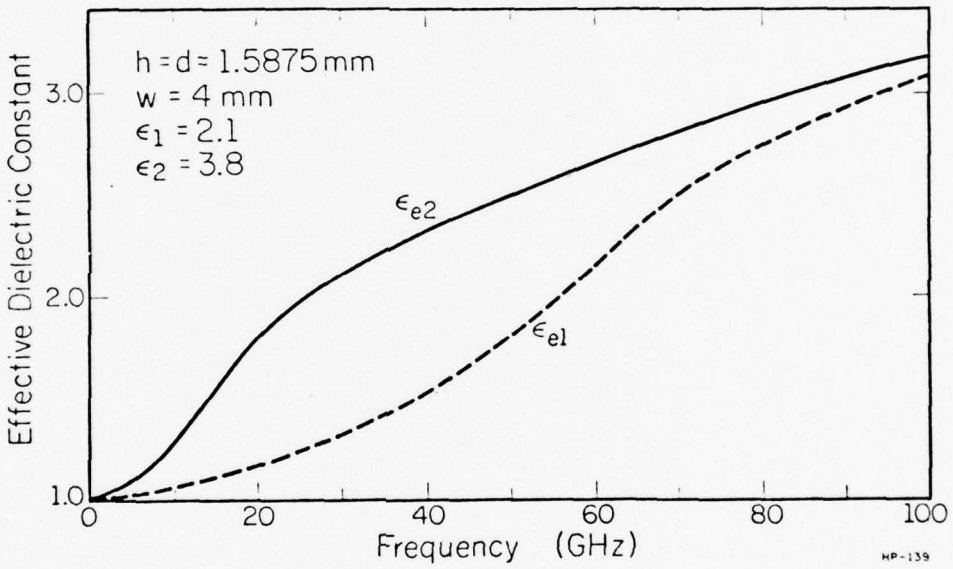

Figure 7. Effective dielectric constant as a function of frequency for a typical heterogeneous inverted strip guide.

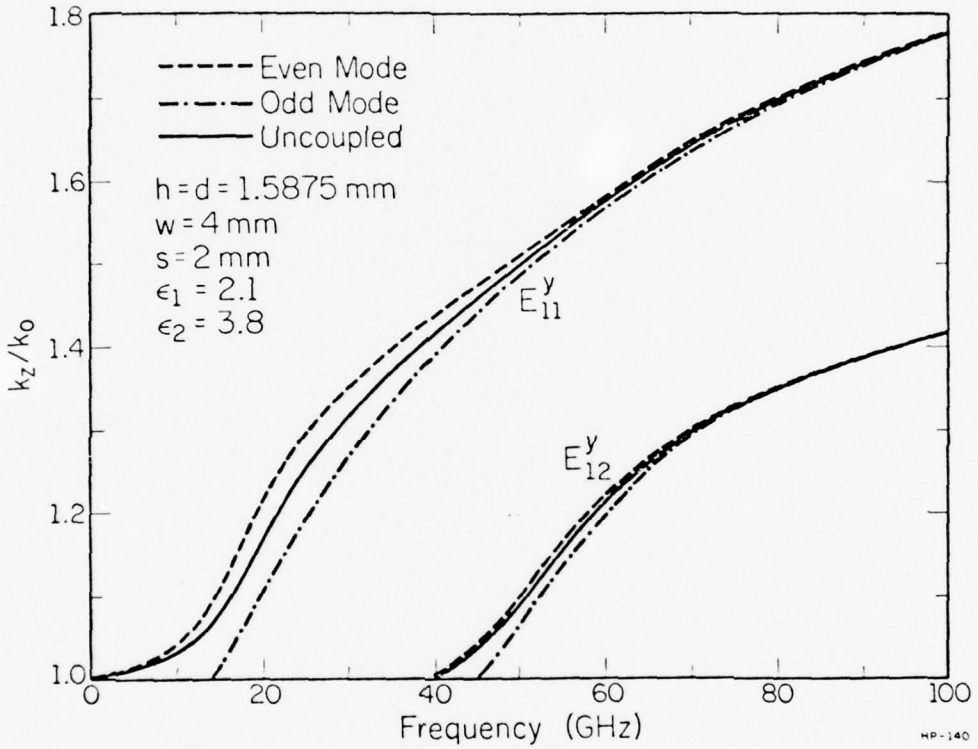

Figure 8. Relative propagation constant as a function of frequency for the uncoupled guide and the even and odd modes of the coupled guide.

s, Figure 9. If we assume that Port 1 is excited, the fields along the coupled guide become:

for $z = 0$

$$E_I(0) = E_1 \qquad \text{Eq 47}$$

$$E_{II}(0) = 0 \qquad \text{Eq 48}$$

for $0 < z < \ell$.

$$E_I(z) = E_e e^{-jK_e z} + E_o e^{-jK_o z} \qquad \text{Eq 49}$$

$$E_{II}(z) = E_e e^{-jK_e z} - E_o e^{-jK_o z} \qquad \text{Eq 50}$$

where $E_I(z)$ and $E_{II}(z)$ are the fields along guides I and II, E_o and E_e are the fields in the odd and even modes of the coupled guide and K_o and K_e are the propagation constants for the odd and even modes. Coupling is the ratio of the power in guides II and I at $z = \ell$.

$$\frac{P_3}{P_2} = \left(\frac{E_{II}(\ell)}{E_I(\ell)} \right)^2 \qquad \text{Eq 51}$$

If the coupler is symetric about the z axis

$$E_e = E_o \qquad \text{Eq 52}$$

Taking the ratio of equations 49 and 50

$$\frac{E_{II}(z)}{E_I(z)} = -j \ \text{TAN}\left[(K_e - K_o)\frac{z}{2}\right] \qquad \text{Eq 53}$$

Squaring Equation 53 we obtain the coupling at any point z.

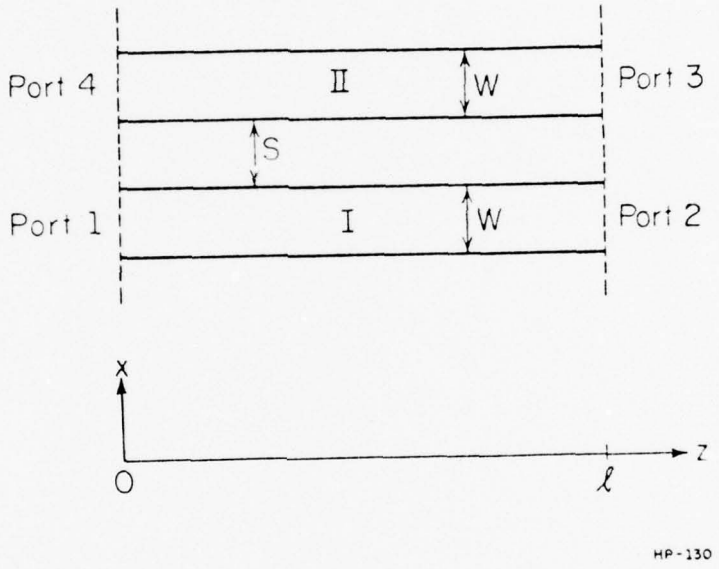

Figure 9. Isolated distributed directional coupler.

$$\frac{P_3(z)}{P_2(z)} = \text{TAN}^2\left[(K_e - K_o)\ \frac{z}{2}\right] \qquad \text{Eq 54}$$

We note that the coupling is periodic with respect to z with a periodicity of L/2 where L is

$$L = \frac{\pi}{(K_e - K_o)} \qquad \text{Eq 55}$$

Using L, the coupling is written as

$$\frac{P_3}{P_2} = \text{TAN}^2\left(\frac{\pi \ell}{2L}\right) \qquad \text{Eq 56}$$

For a typical guide, L versus frequency is shown in Figure 10 using various line separations, s.

A practical coupler of this type is shown in Figure 11. In a practical coupler there is a significant amount of coupling due to the connecting guides. Provided the coupler is symetric about the x-axis, at its midpoint, we may define the quantity

$$\Delta\phi = 2 \int_{Z_o}^{Z'} [K_e(z) - K_o(z)]\, dz \qquad \text{Eq 57}$$

where z' is some value of z at which $K_e(z) \simeq K_o(z)$. Equation 57 is simply a more general form of the denominator of Equation 55. Rewriting Equation 56 to take into account coupling due to the connecting guides

$$\frac{P_3}{P_2} = \text{TAN}^2\left[\frac{\pi \ell}{2L} + \frac{\Delta\phi}{2}\right] \qquad \text{Eq 58}$$

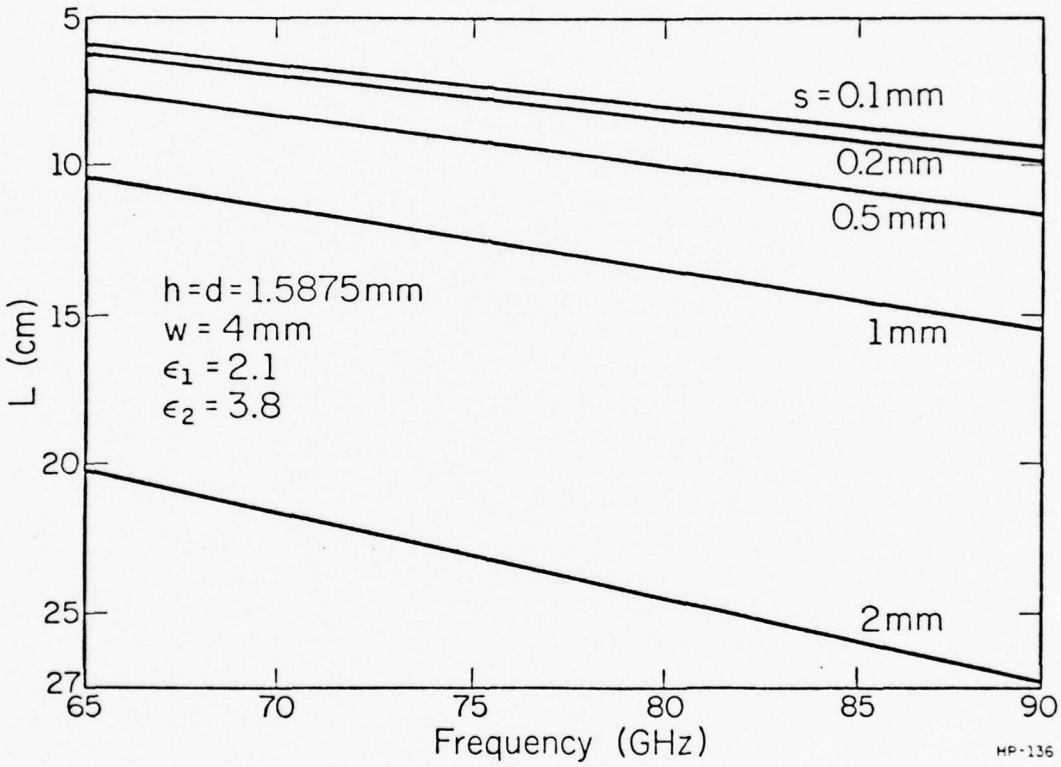

Figure 10. Coupling length as a function of frequency for typical line separations.

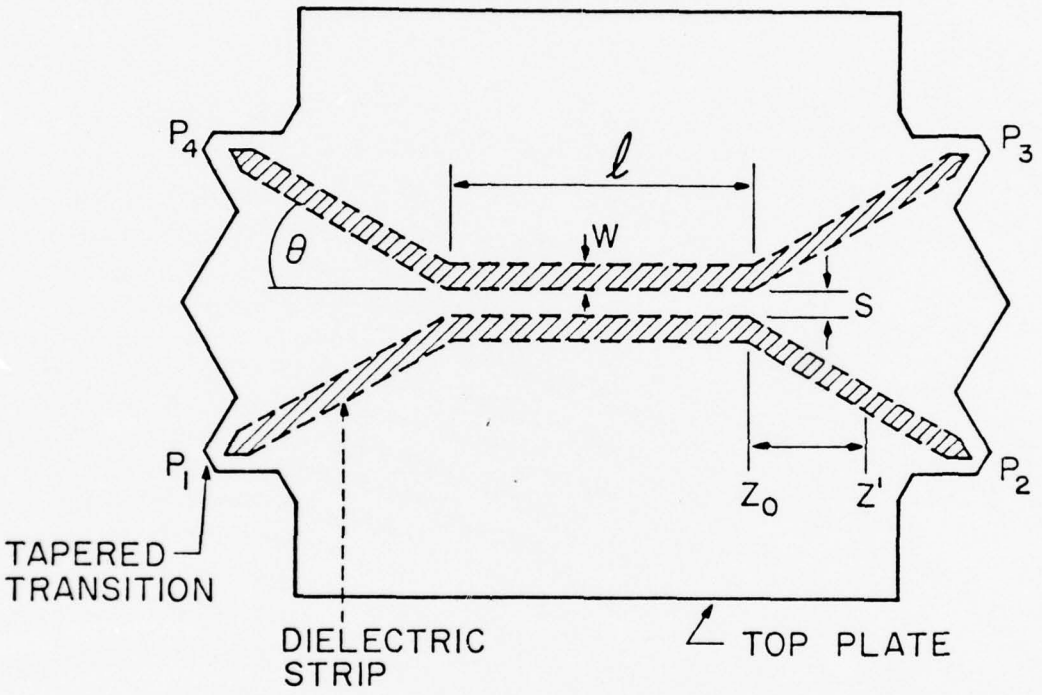

Figure 11. Top view of the directional coupler showing the four connecting guides.

5. Analysis of the Beam Splitter Directional Coupler

Using inverted strip guide a directional coupler analogous to the optical beam splitter is possible. The coupler consists of two perpendicularly intersecting guides in which a gap, oriented at 45° to each guide, is made in the guiding strips (Figure 12). In the gap the effective dielectric constant is ε_{RI}, corresponding to the top plate floating above the ground plane, while in the regions containing the guiding strip the effective dielectric constant is ε_{RII}.

As a first order approximation, the phase front of the dominant mode in the inverted strip guide is similar to that of a plane wave. The coupler can be modeled as a semi-infinite structure as in Figure 12b. Using this structure the reflection coefficient, ρ, for the E_y^{pq} modes, due to the discontinuity at the gap, can be found.

From transmission line theory (Figure 12c).

$$\rho = \frac{E_r}{E_i} = \frac{Z_{in} - Z_1}{Z_{in} + Z_1} \qquad \text{Eq 59}$$

where E_r is the magnitude of the reflected E field and E_i is the magnitude of the incident E field. The input impedance at interface 1 is

$$Z_{in} = Z \left(\frac{Z_1 + j Z_2 \beta_2 s}{Z_2 + j Z_1 \beta_2 s} \right) \qquad \text{Eq 60}$$

where

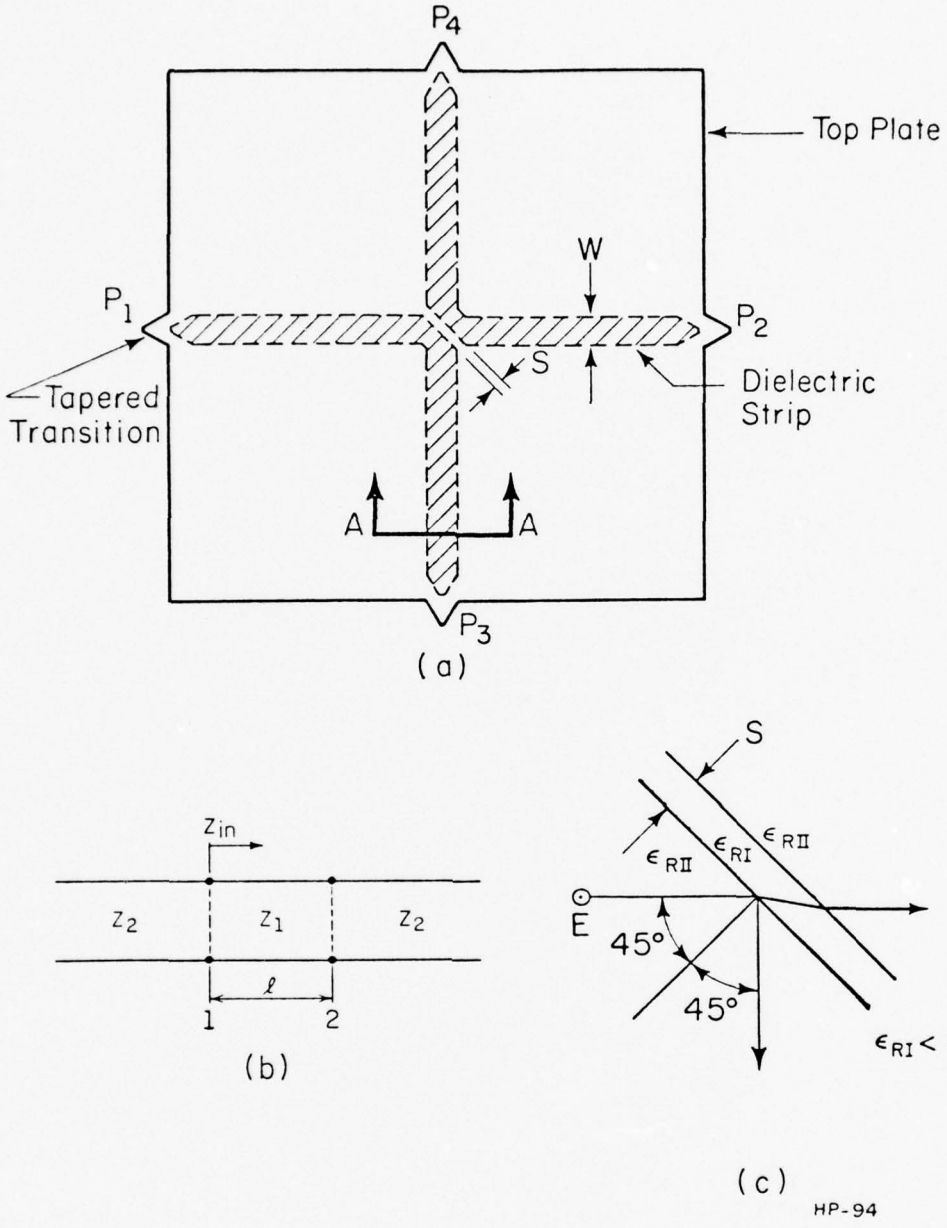

Figure 12. Beam splitter type directional coupler
(a) Top view.
(b) Equivalent model using plane wave assumption.
(c) Representation of 12b in terms of transmission line concepts.

$$\beta_2 = \sqrt{\varepsilon_{RII}}\, k_o \quad \text{COS } \phi \qquad \text{Eq 61}$$

Using Snell's Law

$$\sqrt{\frac{\varepsilon_{RI}}{2}} = \sqrt{\varepsilon_{RII}} \quad \text{SIN } \phi \qquad \text{Eq 62}$$

β_2 may be written as

$$\beta_2 = \sqrt{\varepsilon_{RII}}\, k_o \left(1 - \frac{\varepsilon_{RI}}{2\varepsilon_{RII}}\right) 1/2 \qquad \text{Eq 63}$$

The characteristic impedences of each section are:

$$Z_1 = \frac{2\eta_1}{\sqrt{2}} = \sqrt[2]{\frac{\mu_o}{2\varepsilon_o \varepsilon_{RII}}} \qquad \text{Eq 64}$$

$$Z_2 = \eta_2 \text{ SEC } \phi = \sqrt{\frac{\mu_o}{\varepsilon_o \varepsilon_{RII}}} \left(1 - \frac{\varepsilon_{RI}}{2\varepsilon_{RII}}\right)^{-1/2} \qquad \text{Eq 65}$$

Defining the variables:

$$q = \sqrt{\frac{\varepsilon_{RI}}{\varepsilon_{RII}}} \qquad \text{Eq 66}$$

$$p = \sqrt{2 - \left(\frac{\varepsilon_{RI}}{\varepsilon_{RII}}\right)} \qquad \text{Eq 67}$$

and

$$\alpha = \frac{q}{p} = \frac{Z_2}{Z_1} \qquad \text{Eq 68}$$

and substituting into Equation 60

$$\frac{Z_{in}}{Z_1} = \frac{1 + j\ \alpha\ \mathrm{TAN}(\beta_2 s)}{1 + j\ 1/\alpha\ \mathrm{TAN}(\beta_2 s)} \qquad \text{Eq 69}$$

Rewriting ρ as

$$\rho = \frac{\frac{Z_{in}}{Z_1} - 1}{\frac{Z_{in}}{Z_1} + 1} = \frac{j(\alpha - 1/\alpha)\ \mathrm{TAN}(\beta_2 s)}{2 + j\ (\alpha + 1/\alpha)\ \mathrm{TAN}(\beta_2 s)}$$

Eq 70

Squaring equation 70 the power reflection coefficient becomes:

$$\frac{P_3}{P_1} = |\rho|^2 = \frac{(\alpha - 1/\alpha)^2\ \mathrm{TAN}^2(\beta_2 s)}{4 + (\alpha + 1/\alpha)\ \mathrm{TAN}^2(\beta_2 s)} \qquad \text{Eq 71}$$

where the energy is reflected into the output port, P_3, from the input port, P_1. This type of coupler would normally be used when fairly small coupling is desired. Typically, about 1% of the input energy is coupled into the output port. In terms of the gap width, s, and effective dielectric constants the coupling becomes:

$$\frac{P_3}{P_1} = \frac{(\alpha - \frac{1}{\alpha})^2\ \mathrm{TAN}^2\left(K_o\ sp\ \sqrt{\frac{\varepsilon_{RI}}{2}}\right)}{4 + (\alpha + \frac{1}{\alpha})^2\ \mathrm{TAN}^2\left(K_o\ sp\ \sqrt{\frac{\varepsilon_{RI}}{2}}\right)}$$

Eq 72

Equation 72 is plotted as a function of frequency for various gap sizes in Figure 13.

6. Analysis of the Ring Resonator

Using inverted strip guide a simple resonator may be fabricated by simply constructing a closed ring with the guiding layer, Figure 20, page 44.

For the ring resonator resonance occurs when

$$n \lambda_g = 2\pi\bar{r} \qquad \text{Eq 73}$$

where λ_g in the wavelength in the ring and $\bar{r}$ is the effective radius of the ring. If the width of the ring is small compared to the radius

$$\bar{r} \sim \sqrt{ab} \qquad \text{Eq 74}$$

where a and b are the outer and inner radii of the ring.

When the radius of curvative is large, mutual coupling in the ring may be neglected, λ_g may be approximated by the guide wavelength in a straight section of inverted strip guide. The resonant frequencies are then easily calculated using equation 73.

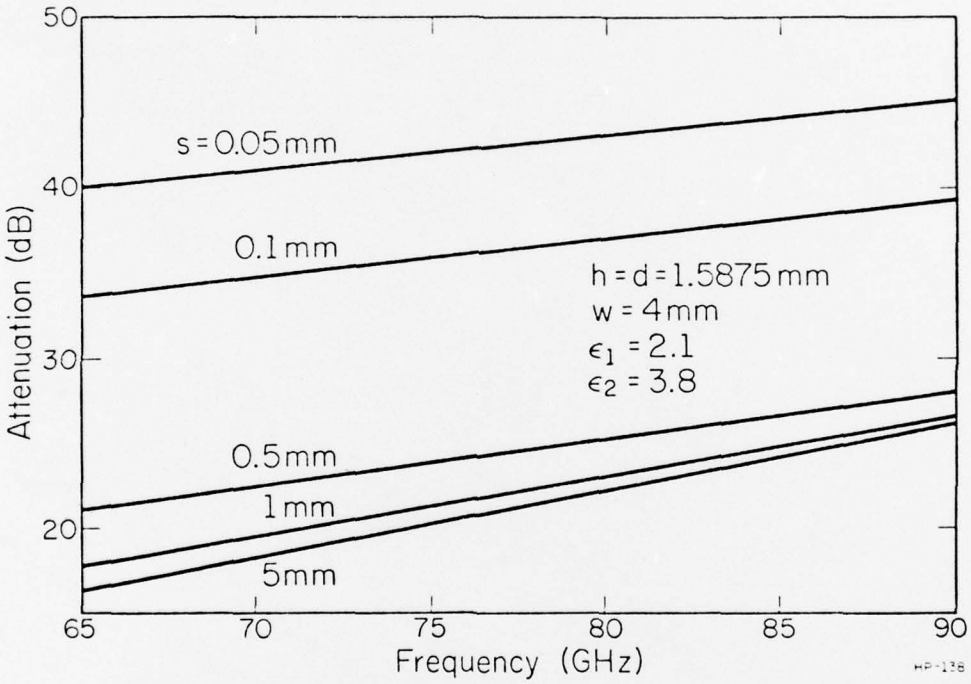

Figure 13. Relative energy coupled into the output port as a function of frequency for typical gap widths.

CHAPTER III

EXPERIMENTAL PROCEDURE AND RESULTS

The experiments were conducted with the single objective of testing the theory with which the devices were analyzed. Little was done to minimize VSWR, maximize resonator Q or other optimizations important in practical applications. The following results must be interpreted with these points in mind.

A Hughes 41253H, E band, micrometer tuned, impatt oscilator with integral isolator is used as a source for all experiments. Using RG 99/U waveguide a simple system consisting only of the Hughes oscilator, a TRG E130 modulator, and a Systron Donner DBH-319 (IN53-diode) detector was used for all measurements. Initially a fairly elaborate system which additionally included 2 TRG directional couplers, a Hitachi ferrite isolator, tuned cavity (for frequency monitoring) and an additional Systron-Donner detector was used. The combined nonlinearities of the above components over the 5GHz bandwidth used in the experiments proved to great to produce any useful information. Even with the simpler system all data had to be presented as the ratio of signal measured with the device under test and signal measured with a control. This minimized the effects of the variation of oscilator output as a function of frequency. An HP 415E SWR meter was used to measure the relative power output.

Figure 14 shows the tapered transition used for the metal to dielectric guide transition. As an input transition this method was fairly successful but when used as an output transition to a detector a fairly high VSWR is produced on the dielectric guide because of the mismatch at the transition. Attempts at minimizing this mismatch by lengthening the taper were unsuccessful because of the brittleness of the quartz.

Figure 15 shows the experimental results for the directional coupler shown in Figure 16. Very likely there is scattering or diffraction (mismatch) at the junctions between the isolated coupler and the connecting guides. This effect could account for the additional coupling that was measured. This same effect could contribute to the degradation of directivity (power at port 4) but the major component of the power at port 4 is due to reflection at ports 2 and 3 because of the tapered transitions.

Data for the beam splitter type directional coupler is shown in Figures 17 and 18. The high VSWR along the guide tends to mask the performance of the coupler itself.

The performance of the ring resonator is shown in Figure 19. Initially port 1 was directly across from port 2, Figure 20. In this configuration there was sufficient energy propagating along the surface of the quartz plate, to port 2, to completely mask any resonances. With the 90° orientation, as shown in Figure 19, the input port excites both odd and even order resonances while the output port

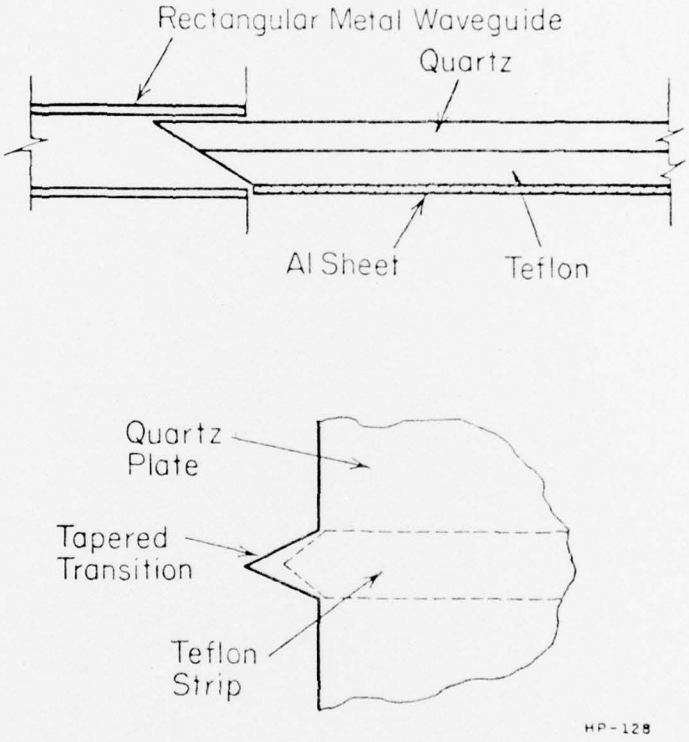

Figure 14. Side and top views of the metal to dielectric tapered transition.

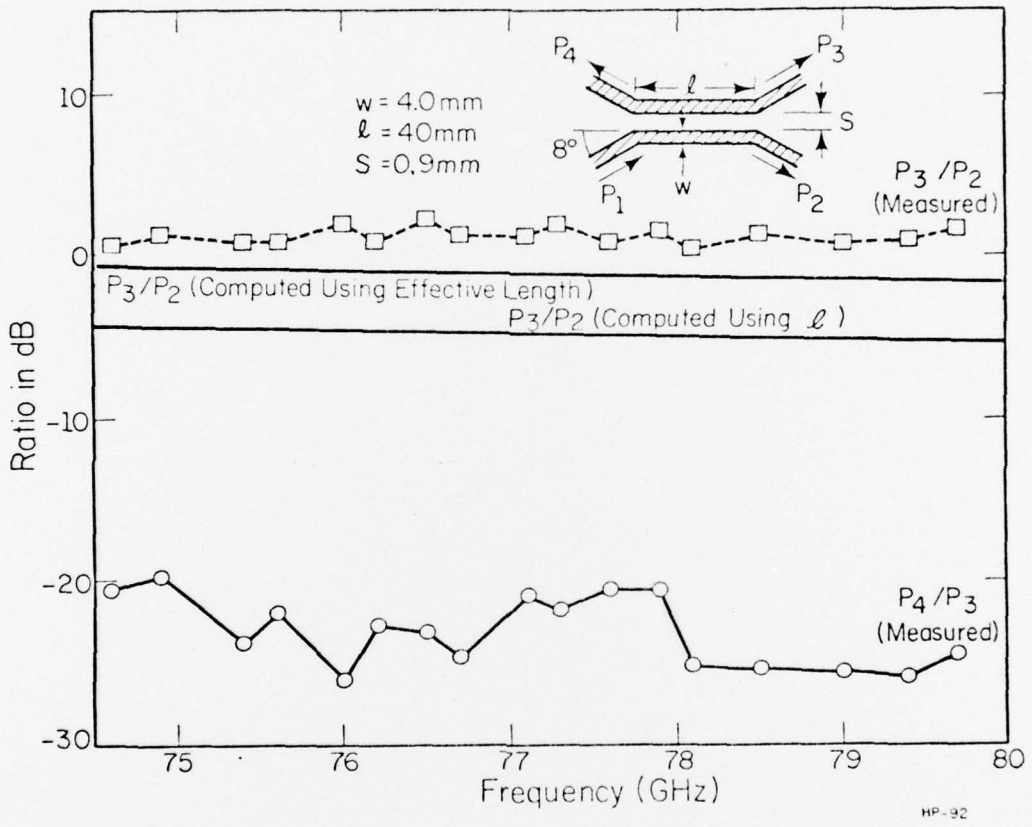

Figure 15. Comparison of numerical and experimental results for the distributed directional coupler.

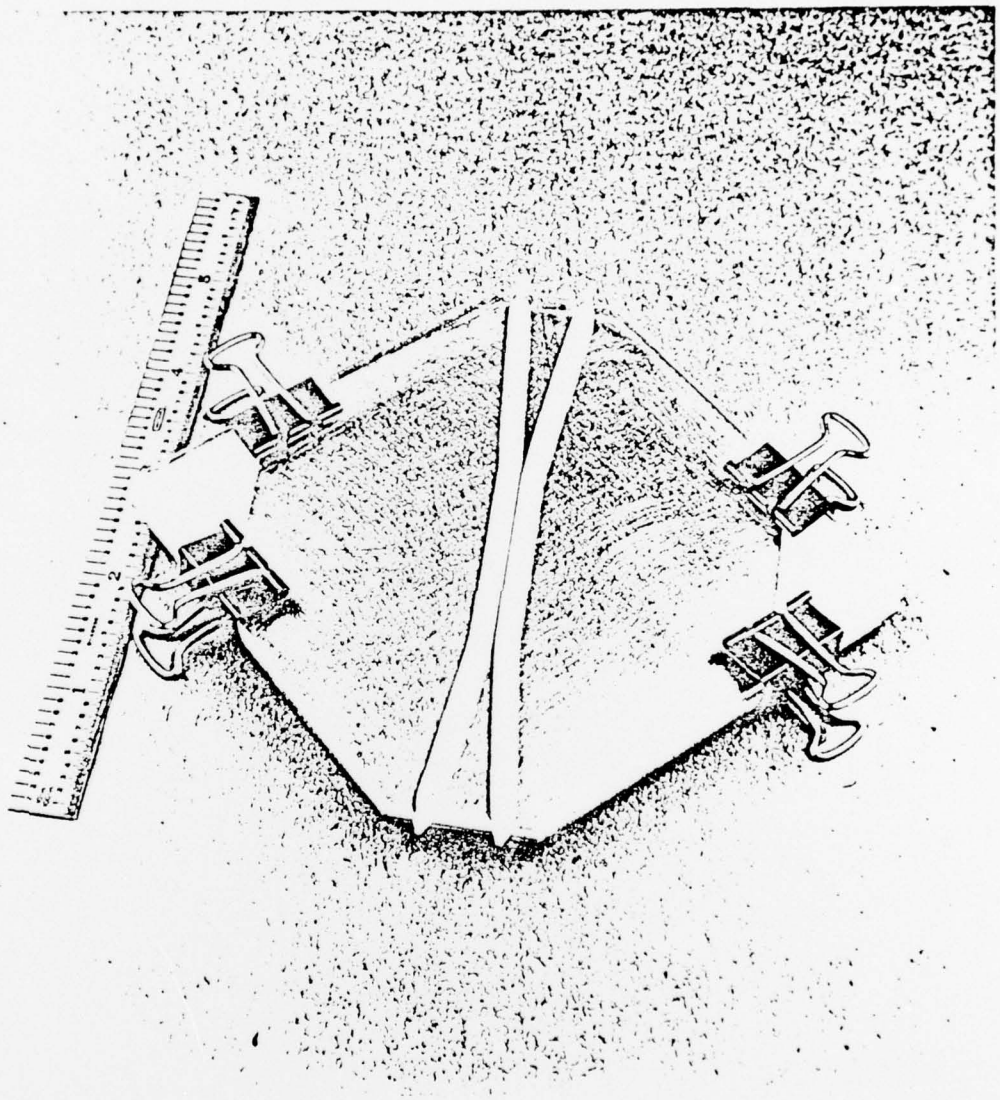

Figure 16. The distributed directional coupler.

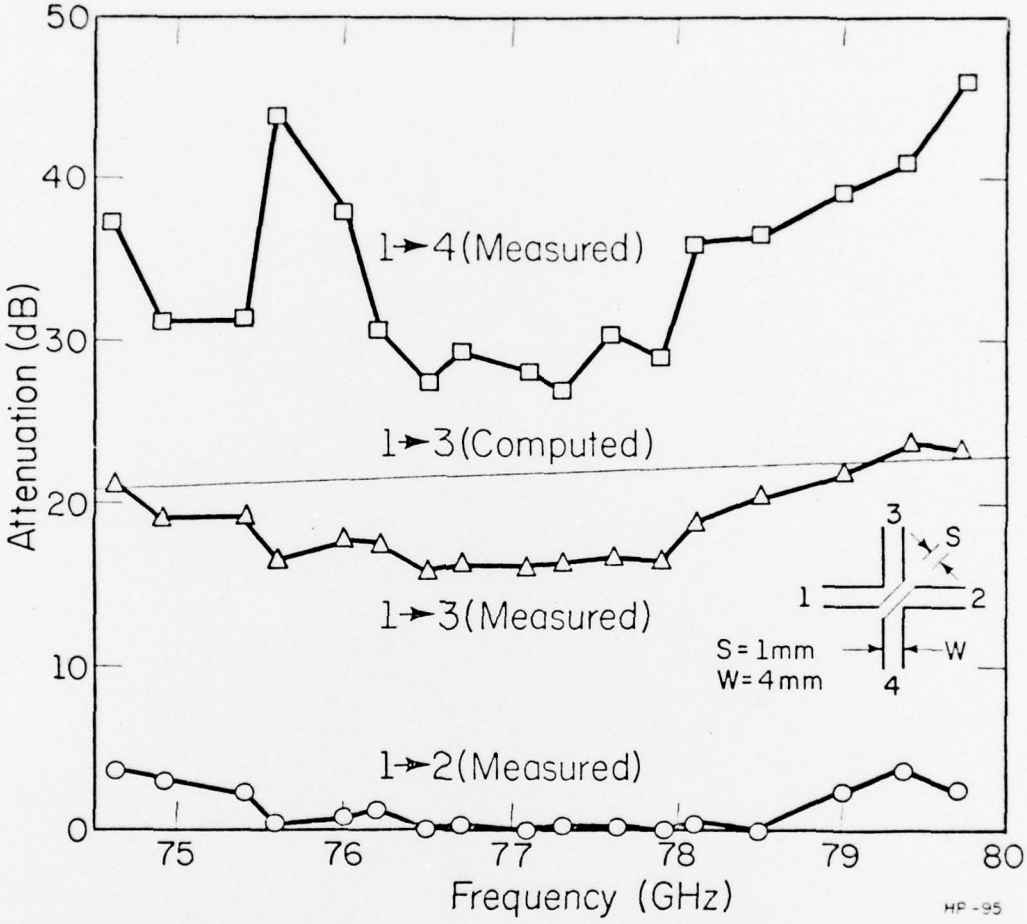

Figure 17. Comparison of numerical and experimental results for the beam splitter type directional coupler.

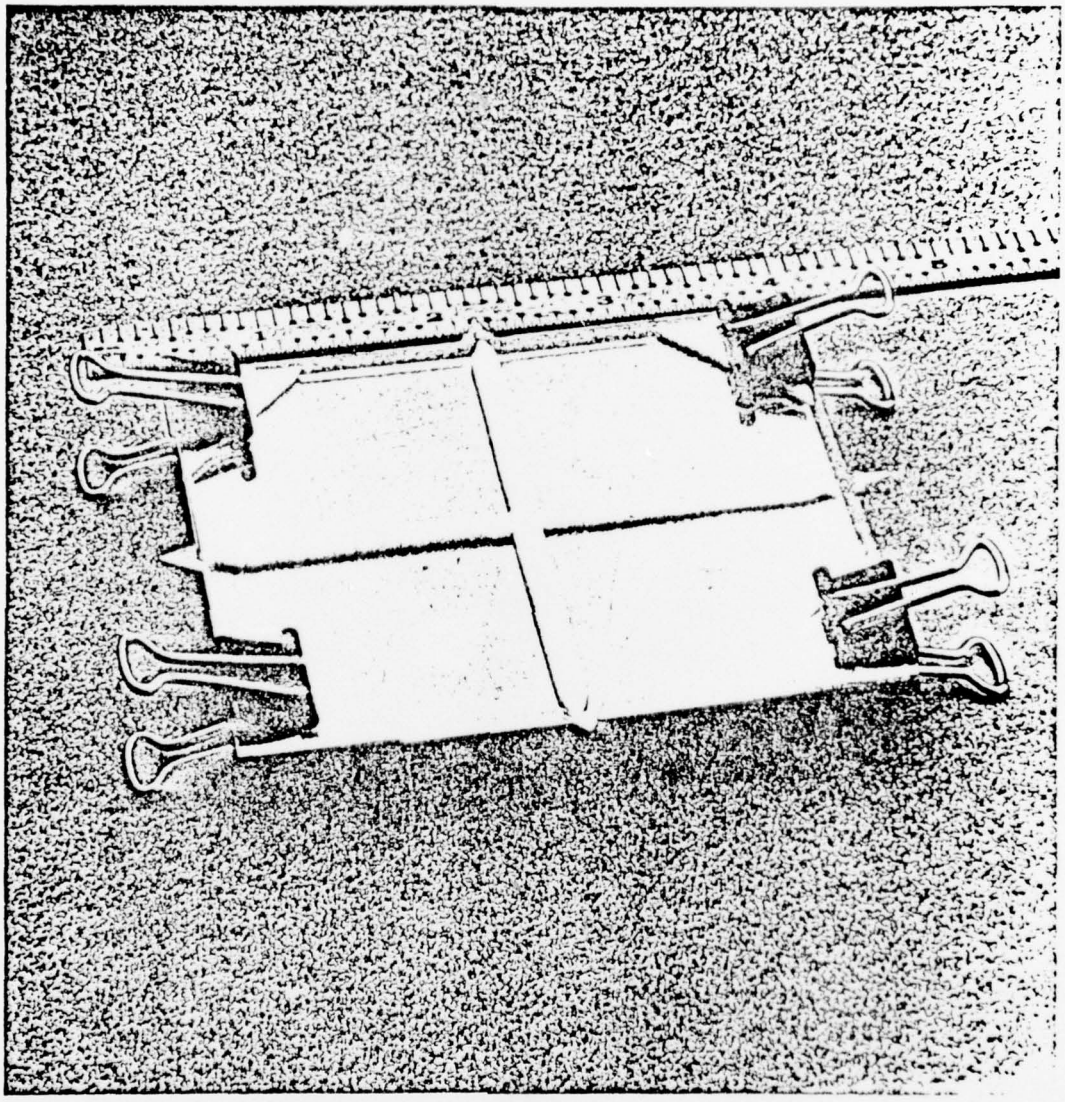

Figure 18. The beam splitter type directional coupler.

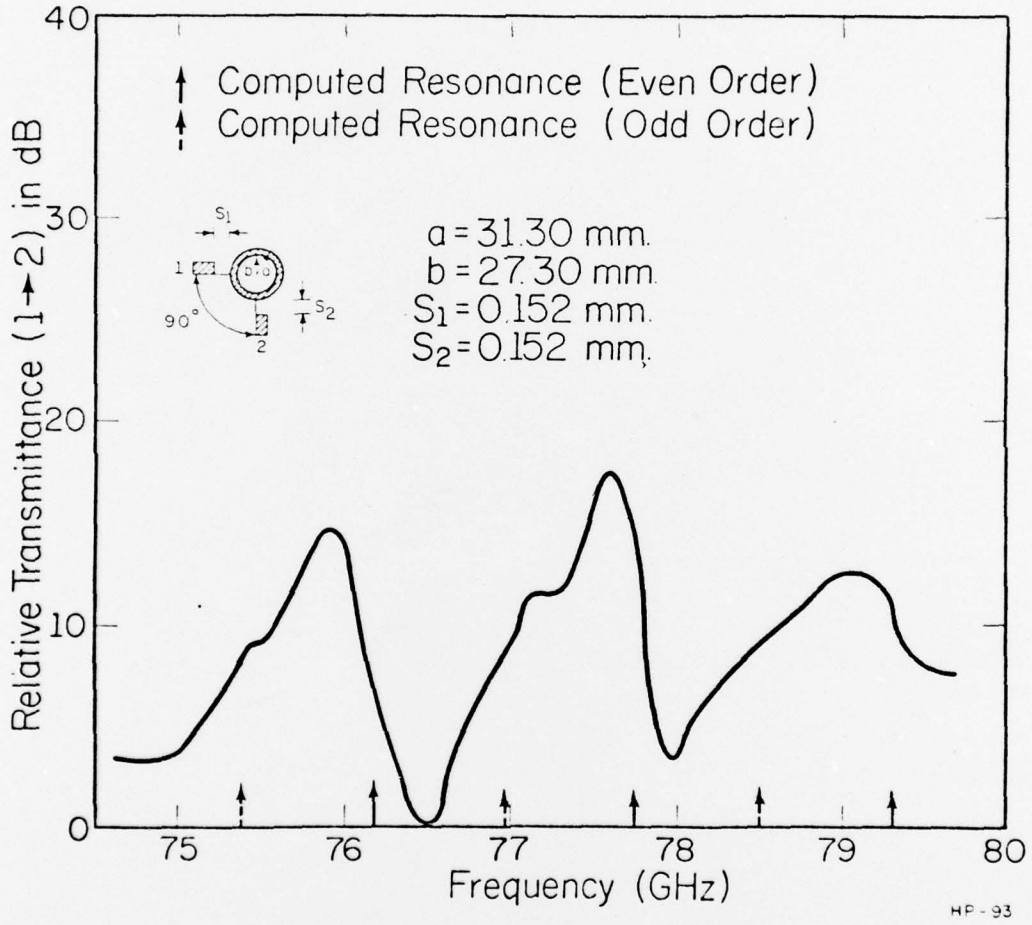

Figure 19. Performance of the ring resonator.

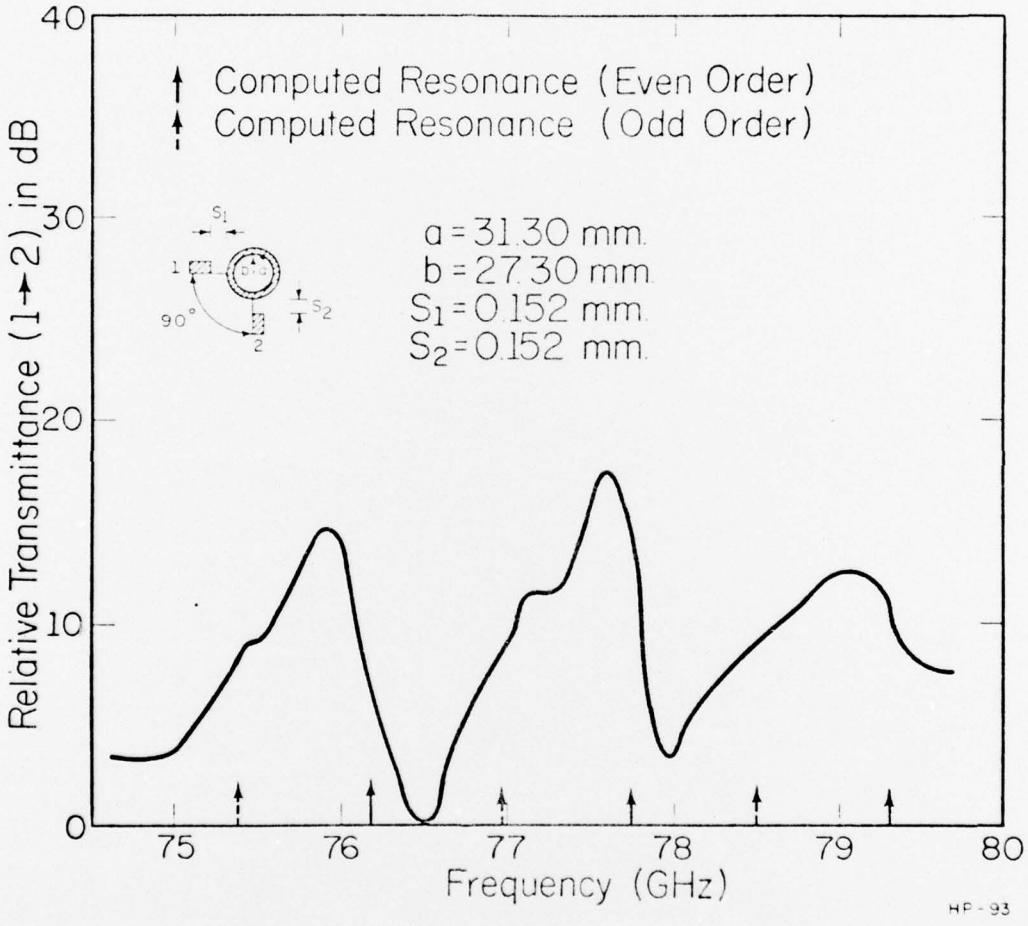

Figure 19. Performance of the ring resonator.

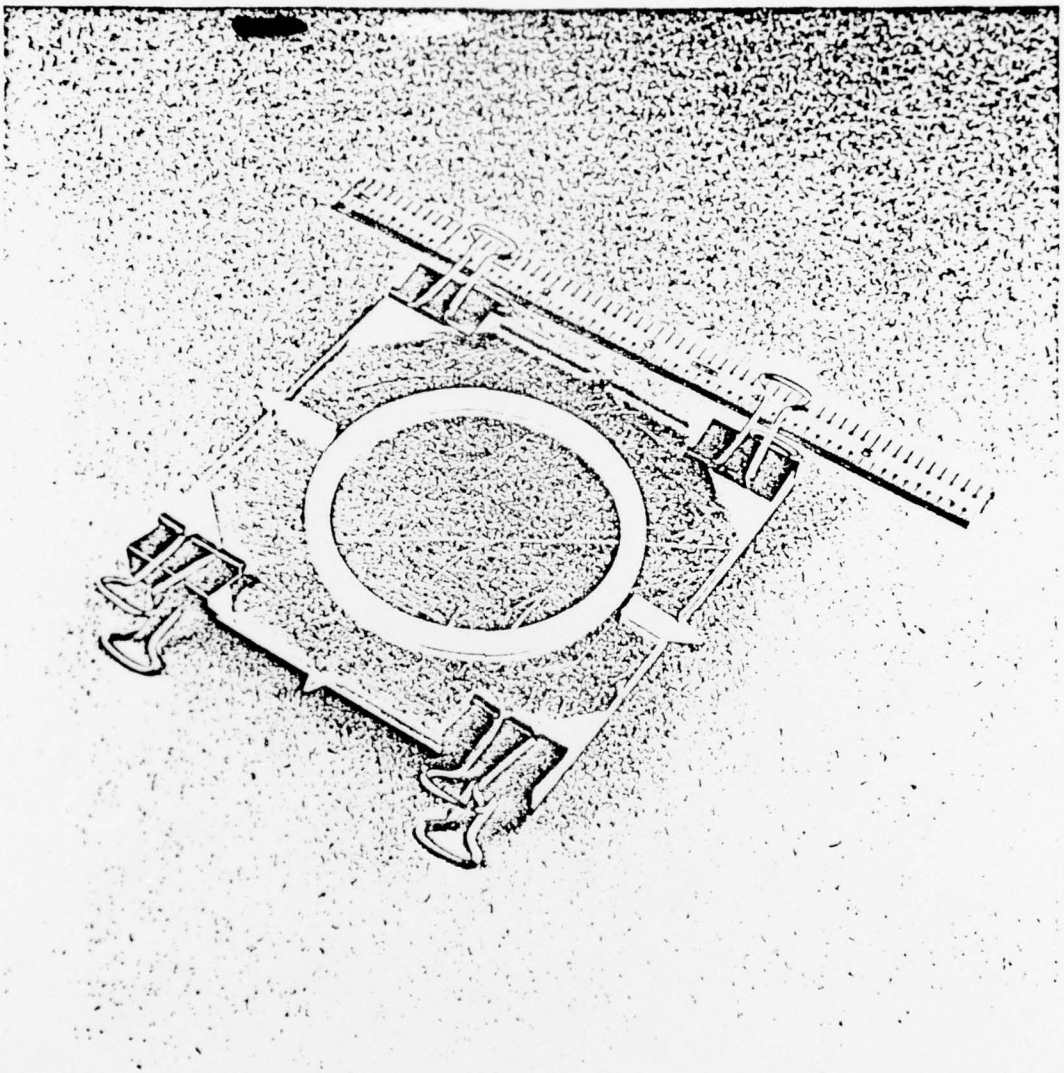

Figure 20. Ring resonator.

can only be excited by the even order resonances since it is placed at a null for the odd order resonances. In Figure 19 we see that the strongly coupled even order resonances are shifted about .2 GHz towards the lower frequencies while the weakly coupled odd order resonances remain essentially unshifted.

CHAPTER IV

CONCLUSIONS

Several passive components for millimeter wave integrated circuits have been analyzed and demonstrated. Agreement between calculations and experiments has been good. The results derived from fairly simple analysis and numerical methods used have been found to give good correlation with experiments.

Concerning the materials used, quartz and teflon, because of the fabrication and handling problems of quartz it would be more practical to use a more durable material. This brings to mind an all teflon guide which would have characteristics very similar to those of the quartz-teflon guide. Preliminary experiments have been done with a homogeneous guide using a plastic of dielectric constant 4.0 (powdered titanium dioxide dispensed in a plastic carrier). Comparison of calculated and measured field distributions are very good.

LIST OF REFERENCES

1. E. A. J. Marcatili, "Dielectric Rectangular Waveguide and Directional Coupler for Integrated Optics," Bell System Technical Journal, Vol. 48, No. 7, pp. 2079-2102, September 1969.

2. J. E. Goell, "A Circular-Harmonic Computer Analysis of Rectangular Dielectric Waveguides," Bell System Technical Journal, Vol. 48, No. 7, pp. 2133-2160, September 1969.

3. R. M. Knox and P. P. Toulios, "Integrated Circuits for the Millimeter Through Optical Frequency Range," Proceedings of the Symposium on Submillimeter Waves, New York, New York, March 31, April 1 & 2, 1970.

4. D. Marcuse, Theory of Dielectric Optical Waveguides, Academic Press, Inc., New York, 1974.

5. R. F. Harrington, Time-Harmonic Electromagnetic Fields, McGraw-Hill Book Company, Inc., New York, 1961.

6. W. V. McLevige, Tatsuo Itoh and Raj Mittra, "New Waveguide Structures for Millimeter-Wave and Optical Integrated Circuits," IEEE Transactions on Microwave Theory and Techniques, Vol. MTT-23, No. 10, October 1975, pp. 788-794.

7. R. M. Knox, "Dielectric Waveguide: A Low-Cost Option For ICS," Microwaves, March 1976, pp. 56-67.

8. R. Rudokas and T. Itoh, "Passive Millimeter-Wave IC Components Made of Inverted Strip Dielectric Waveguide," IEEE Transactions on Microwave Theory and Techniques - Special Issue on 1976 Symposium, to be published.

9. S. E. Miller, "Coupled Wave Theory and Waveguide Applications," The Bell System Technical Journal, May 1954, pp. 661-719.

10. H. F. Taylor, "Power Loss at Directional Change in Dielectric Waveguides," Applied Optics, Vol. 13, No. 3, March 1974, pp. 642-647.

11. T. Itoh, "Inverted Strip Dielectric Waveguide for Millimeter-Wave Integrated Circuits," IEEE Transactions on Microwave Theory and Techniques, Vol. MTT-24, No. 11, November 1976.